Reconstruction of the photon distribution in a micromaser

S. Olivares[1,2(a)], F. Casagrande[1(b)], A. Lulli[1(c)] and M. G. A. Paris[1,3,4(d)]

[1] *CNISM, UdR Milano Università - I-20133 Milano, Italia*
[2] *Dipartimento di Fisica e Matematica dell'Università dell'Insubria - I-22100 Como, Italia*
[3] *Dipartimento di Fisica dell'Università di Milano - I-20133 Milano, Italia*
[4] *Institute for Scientific Interchange Foundation - I-10133 Torino, Italia*

Abstract – We suggest an iterative, maximum-likelihood–based, method to reconstruct the photon number distribution of the steady-state cavity field of a micromaser starting from the statistics of the atoms leaving the cavity after the interaction. The scheme is based on measuring the atomic populations of probe atoms for different interaction times and works effectively using a small number of atoms and a limited sampling of the interaction times. The method has been tested by numerically simulated experiments showing that it may be reliably used in any micromaser regime, leading to high-fidelity reconstructions for single-peaked distributions as well as for double-peaked ones and for trapping states.

Introduction. – The one-atom maser or *micromaser* is perhaps the most relevant example of open quantum system in cavity quantum electrodynamics (CQED) [1]. Since its first experimental realization [2] this system has allowed to investigate many fundamental aspects in quantum optics. The micromaser dynamics results from the interplay of a coherent interaction between a beam of two-level atoms and a resonant cavity mode in the microwave domain, as described by the Jaynes-Cummings (JC) model [3], and the dissipative process due to the contact of the cavity with the environment. At the steady state the radiation field inside the high-Q cavity may show highly non-classical features, as for example sub-Poissonian photon statistics [4] or quantum collapses and revivals [5]. In addition, states characterized by a truncated photon number distribution, the so-called *trapping states* (TS) of the cavity field [6], may be generated. These states show up only at very low temperature and may be affected by collective atomic interactions [7]. Under suitable pumping conditions, photon distribution at the steady state may also show two coexisting maxima, that is the signature of first-order phase-transitions [8].

Operating the micromaser under pulsed regime and trapping conditions the generation of Fock states has been also reported [9]. A micromaser was implemented also on a two-photon transition [10] and more recently a microlaser was operated in the optical regime [11].

A crucial aspect of the micromaser is that, in order to preserve high-Q values of the cavity, the cavity field is not accessible to direct measurements. As a consequence, any information on its properties must be inferred from the atoms leaving the cavity after the interaction. In fact, the relation between the atomic statistics and the properties of the cavity field has been theoretically and numerically investigated [12] also including the back-action due to the atomic measurements [13]. On the other hand, to the best of our knowledge, no method has been suggested to reconstruct the whole photon distribution by exploiting the complete information carried by the atoms leaving the cavity. In earlier experiments [4,5] the atomic statistics was obtained by counting the number of excited (ground) atoms in a time interval longer than the cavity lifetime, and then this frequency was compared with the theoretical expression (see below) for the experimental set of parameters. As a matter of fact, the photon distribution was not reconstructed from the measurements. In experiments leading to TS [6] the steady-state photon distribution is composed only by few

terms allowing a simple fit of experimental data, whereas in the experiments to generate Fock states [9] the cavity field state $|n\rangle$ is prepared by a pulse of n pump atoms and only one probe atom is measured to obtain the atomic inversion that ideally involves only one Rabi frequency. In this case, the advantage to measure only one probe atom is that of avoiding the cavity field state reduction due to repeated atomic measurements.

In this letter, we suggest a method to reconstruct the full steady-state photon distribution of the cavity field starting from measurements of the statistics of probe atoms. The basic idea is that atoms leaving the cavity after different interaction times are carrying the complete information about the cavity field itself. Indeed, the method is based on measuring the atomic statistics for different interaction times and then estimating the photon distribution using maximum-likelihood reconstruction. As we will see, the method is very effective in any operating regime of the micromaser and allows reliable reconstructions for single-peaked distributions as well as for multi-peaked ones and for trapping states. Remarkably, the method works effectively starting from the statistics of a small number of atoms and a limited sampling of the interaction times. As a consequence, the atoms used to probe the cavity field are only slightly perturbing the steady-state, which itself depends on the interaction time of the pump atoms, *i.e.*, the method can be used *on-line* with experiments. We also notice that at the steady-state, the cavity field density matrix is diagonal in the Fock number basis, and thus the reconstruction of the photon distribution corresponds to the full quantum state reconstruction. On the other hand, the characteristics of the micromaser spectrum [14] are related to the decay of off-diagonal elements of the cavity field density matrix in the transient regime.

Photon distribution at the steady state. – A schematic diagram of the micromaser setup is given in fig. 1 where a beam of two level atoms, excited in the upper Rydberg level of the maser transition, continuously and resonantly pump a high-Q microwave cavity mode. The cavity temperature is kept as low as $0.5\,\mathrm{K}$ in order to have a small mean thermal photon number n_{th}. The velocity of the atoms can be selected so that the interaction time t_{int} between each atom and the cavity mode can be selected with high precision. The atomic flux has a Poissonian distribution with a mean pump rate R. The state of the atoms leaving the cavity can be detected by field ionization techniques.

The atomic decay rate γ_a and the cavity decay rate γ are taken such that $t_{\mathrm{int}} \ll R^{-1} \ll \gamma^{-1} \ll \gamma_a^{-1}$. Under the above conditions only one atom interacts with the cavity mode each time, thus realizing a perfect JC interaction. The cavity field dynamics, including dissipation effects, can be described by a Master equation and a steady-state regime can be obtained. If ϱ_{F} denotes the (diagonal) steady-state density operator of the cavity field,
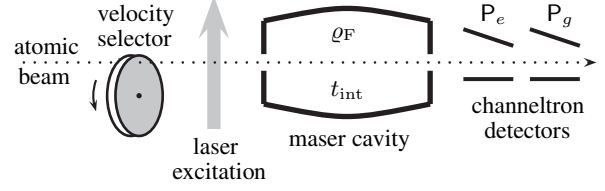

Fig. 1: Schematic diagram of the micromaser setup.

the photon distribution $p_n \equiv p_n(\Theta_{\mathrm{int}}, N_{\mathrm{ex}}, n_{\mathrm{th}}) = \langle n|\varrho_{\mathrm{F}}|n\rangle$ can be expressed as [8]

$$p_n = p_0 \prod_{m=1}^{n} \frac{(N_{\mathrm{ex}}/m)\sin^2\left(\Theta_{\mathrm{int}}\sqrt{m/N_{\mathrm{ex}}}\right) + n_{\mathrm{th}}}{1 + n_{\mathrm{th}}}, \quad (1)$$

where p_0 is a normalization constant, $N_{\mathrm{ex}} = R/\gamma$ the effective pump rate, and $\Theta_{\mathrm{int}} \equiv g t_{\mathrm{int}}\sqrt{N_{\mathrm{ex}}}$ the dimensionless pump parameter, g being the atom-cavity coupling constant.

A striking consequence of eq. (1) is the existence of trapping states of the cavity field [6]. In the limit of $n_{\mathrm{th}} \to 0$ the distribution p_n vanishes at photon numbers n_q ($q = 1, 2, \ldots$) such that $\Theta_{\mathrm{int}} \equiv q\pi\sqrt{N_{\mathrm{ex}}/(1 + n_q)}$. The TS correspond to narrow dips which appear in the stationary mean photon number $\langle N \rangle = \sum_n n p_n$ as a function of the pump parameter Θ_{int}. Another interesting form of p_n can be obtained if the pump parameter is set to $\Theta_{\mathrm{int}} \cong \frac{\pi}{2}$ corresponding to the maximum amplification (MA) regime of the micromaser. In this case, p_n has a shape like that of a coherent state with the same mean photon number. Finally, close to $\Theta_{\mathrm{int}} = 2\pi$ and multiples thereof, the photon distribution p_n assumes a double-peaked (DP) structure corresponding to a first-order phase transition [1,8].

When the system is at steady-state, the probability to find one atom in the excited state after its interaction with the cavity field for a time t_k is given by

$$\mathsf{P}_k = \sum_{n=0}^{\infty} c_{kn}\, p_n, \qquad c_{kn} = \frac{1 + \cos\left(\tau_k\sqrt{n+1}\right)}{2} \quad (2)$$

where $\mathsf{P}_k \equiv \mathsf{P}_e(\tau_k)$ and $\tau_k = g t_k$, is the dimensionless interaction time. Equation (2) provides a link between the experimentally measurable statistics of the probe atoms and the (inaccessible) photon distribution of the cavity field. Equation (2) is the statistical model to be inverted by the method illustrated in the next section.

Reconstruction of the photon distribution. – At a first sight, eq. (2) seems to provide a scarce piece of information about the photon distribution p_n of the micromaser. However, if the atomic statistics is recorded for a suitable set of values of the interaction times, then the information is enough to reconstruct the full photon distribution. As we will see, the inversion of eq. (2), *i.e.*, the reconstruction of p_n, may be obtained by maximum-likelihood estimation upon a suitable truncation of the Hilbert space.

The reconstruction scheme proceeds as follows: the micromaser is pumped until it has reached the steady state for a fixed set of parameters. Then we stop the atomic pump flux and, in a time much shorter than the cavity photon lifetime γ^{-1}, a probe atom prepared in the excited state is sent through the cavity. The velocity of this probe atom may be adjusted in order to vary the interaction time in a given range. After the interaction with the steady-state cavity field the probe atom is detected. We denote by $f_k = \mathcal{N}_k/N_x$ the experimental frequency of probe atoms found in the excited state after an interaction time τ_k, N_x being the total number of probe atoms sent through the cavity with the same interaction time τ_k. Of course, since atom detection modifies the cavity field state, every probe atom is followed by pump atoms to restore the steady-state field. In the following, we assume that the values of interaction times for the probe atoms τ_k, $k = 0, \ldots, n_\tau$ are uniformly distributed between a minimum value τ_0 and a maximum one τ_{n_τ}, which, in turn, are determined by the maximum and minimum velocities allowed by the specific experimental implementation.

Equation (2) is a statistical model for the parameters p_n that can be solved by the maximum-likelihood (ML) estimation. We assume that the photon distribution can be truncated at the $\tilde{n}$-th term (*i.e.*, p_n is negligible for $n > \tilde{n}$) and, without loss of generality, that N_x is independent of k. The global probability of the sample, *i.e.*, the log-likelihood (with normalized P_k) of the detected data reads as follows:

$$\mathsf{L} = \frac{1}{N_x} \log \prod_k \left(\frac{\mathsf{P}_k}{\sum_m \mathsf{P}_m} \right)^{\mathcal{N}_k} = \sum_k f_k \log \frac{\mathsf{P}_k}{\sum_m \mathsf{P}_m}. \quad (3)$$

ML estimates of p_n are the values maximizing the log-likelihood L. Since the model is linear and the unknowns p_n are positive the solution can be obtained using an iterative procedure [15–18]. Indeed, the equations $\frac{\partial \mathsf{L}}{\partial p_n} = 0$ can be written as

$$\frac{\sum_l \mathsf{P}_l}{\sum_l f_l} \sum_k \frac{c_{kn}}{\sum_m c_{mn}} \frac{f_k}{\mathsf{P}_k} = 1, \quad \forall n = 0, \cdots, \tilde{n}. \quad (4)$$

Then, by multiplying both sides of eq. (4) by p_n, we get a map $\boldsymbol{T} p_n = p_n$, whose fixed point can be obtained by the following iterative solution:

$$p_n^{(h+1)} = \frac{p_n^{(h)}}{\sum_m p_m^{(h)}} \sum_k \frac{c_{kn}}{\left(\sum_l c_{ln} \right)} \frac{f_k}{\mathsf{P}_k^{(h)}}, \quad (5)$$

where $p_n^{(h)}$ is the value of p_n evaluated at the h-th iteration, and $\mathsf{P}_k^{(h)} = \sum_n c_{kn} p_n^{(h)}$. Equation (5) is usually referred to as the expectation-maximization solution of ML, and is known to converge unbiasedly to the ML solution. As a matter of fact, eq. (5) provides a solution once the initial distribution $p_n^{(0)}$ is chosen. In our simulated experiments we start from the uniform distribution $p_n^{(0)} = (1 + \tilde{n})^{-1}$ in the interval $[0, \tilde{n}]$, though any other distribution $p_n^{(0)}$ such that $\sum_n p_n^{(0)} = 1$, $p_n^{(0)} \neq 0 \; \forall n$, would be appropriate as well. Indeed, the initial distribution is
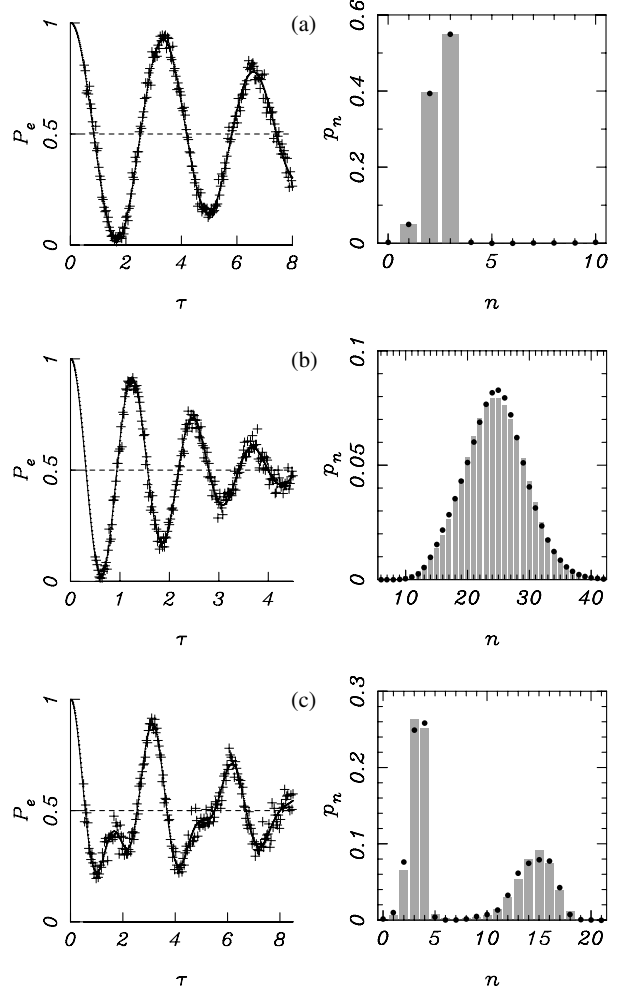

Fig. 2: Reconstruction of the photon number distribution from Monte Carlo simulated experiments for different steady-state micromaser regimes. On the left we report the probability $\mathsf{P}_e(\tau)$ of finding an atom in the excited state as a function of the interaction time τ (as obtained from the reconstructed distribution, solid line) compared with the actual frequencies observed in the simulated experiments (crosses). On the right we show the reconstructed photon distribution (black circles) compared with the theoretical one (histograms). The micromaser parameters are $N_{\text{ex}} = 25.0$, $n_{\text{th}} = 10^{-5}$ and (a) TS regime, $\Theta_{\text{int}}/\pi = 2.5$; (b) MA regime, $\Theta_{\text{int}}/\pi = 0.5$; (c) DP regime, $\Theta_{\text{int}}/\pi = 2.18$. In all the simulated experiments $\tau_0 = 0.5$, $n_\tau = 200$, and $N_x = 200$, $N_{\text{it}} = 1000$.

slightly affecting only the convergence rate and *not* the precision at convergence [19].

Monte Carlo simulated experiments. – Reliability and accuracy of the present method have been tested by an extensive set of numerically simulated experiments, corresponding to different micromaser steady-state regimes. As a figure of merit to assess the accuracy of the reconstructed distribution $p_n^{(\text{r})}$, *i.e.*, the similarity to the actual distribution p_n of eq. (1), we consider the fidelity $G = \sum_n \sqrt{p_n^{(\text{r})} p_n}$. In fig. 2 we show the

Table 1: Mean photon number and Fano factor of the reconstructed distributions of fig. 2 compared with the theoretical values.

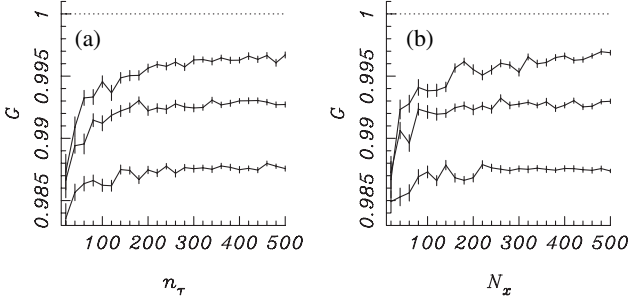|	Θ_{int}	$\overline{n}$	F	$\overline{n}^{(\text{r})}$	$F^{(\text{r})}$	G (%)
TS	$2.5\,\pi$	2.52	0.22	2.53	0.21	99.73
MA	$0.5\,\pi$	24.38	1.02	24.35	1.07	99.43
DP	$2.18\,\pi$	7.85	4.05	7.75	4.08	99.71

Fig. 3: (a): Fidelity of the reconstruction G as a function of the number n_τ of sampling times at fixed number of data $N_x = 200$ for each time value. (b) Fidelity of the reconstruction G as a function of the number N_x of data for each time value at fixed number $n_\tau = 200$ of sampling interaction times. Both plots refer to the case of the TS state, *i.e.*, the reconstruction reported in fig. 2a. In both plots we report the fidelity for different values of the number of iterations N_{it}, from bottom to top: $N_{\text{it}} = 100$, 200 and 1000. The error bars are obtained by averaging over one hundred simulated experiments.

simulated experimental data for the measurement of $\mathsf{P}_e(\tau)$, generated by Monte Carlo technique, and the comparison between the theoretical photon distributions and those obtained by ML estimation. We consider as interesting examples the TS, MA and DP steady-state micromaser regimes. In these regimes the photon number distribution is sub-Poissonian, nearly Poissonian, and super-Poissonian, respectively. In order to better appreciate the accuracy of our reconstruction method we also report (see table 1) the first two moments of the cavity field distribution, *i.e.*, the mean photon number $\overline{n} = \langle a^\dagger a \rangle$ and the Fano factor $F = \left[\langle (a^\dagger a)^2 \rangle - \langle a^\dagger a \rangle^2 \right] / \langle a^\dagger a \rangle$, a being the mode operator of the cavity field and $\langle \cdots \rangle = \text{Tr}\left[\varrho_{\text{F}} \cdots \right]$ denoting the ensemble average. As it is apparent from table 1 a very good agreement is obtained for all the considered regimes between the values obtained from the reconstructed distributions and the actual ones.

Being our reconstruction method based on an iterative solution an important aspect to keep under control is its convergence. In fig. 3 we show the fidelity of the reconstruction as a function of the number n_τ of sampling interaction times and the number N_x of measures for each interaction time, for different numbers of iterations N_{it}.

As it is apparent from fig. 3 the fidelity increases with both n_τ and N_x and it reaches an asymptotic value which
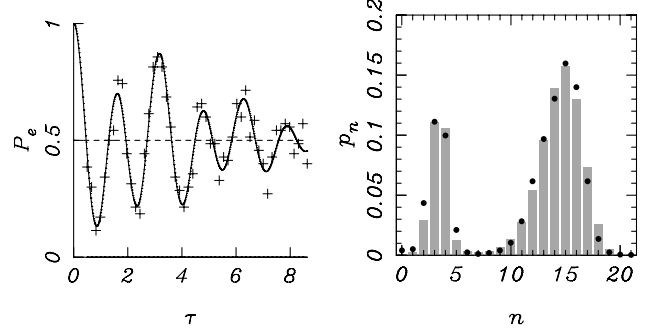

Fig. 4: Reconstruction of the photon number distribution as in fig. 2c but with reduced sampling parameters $N_x = 70$, $n_\tau = 50$, and $N_{\text{it}} = 300$. For these values of parameters we have $\overline{n} = 11.55$, $F = 2.34$, $\overline{n}^{(\text{r})} = 11.23$, $F^{(\text{r})} = 2.50$, and $G = 99.49\%$.

actually depends on the choice of the other parameters. Of course, also the number of iterations N_{it} affects the fidelity value at convergence. Notice, however, that the reconstruction is already very accurate with a number of iterations $N_{\text{it}} = 100$. It is worth noticing that the number of sampling times n_τ cannot be increased at will, since it is limited by experimental constraints. In order to check the statistical reliability of the algorithm we report the results from repeated (simulated) experiments. The error bars in fig. 3 are obtained by averaging over one hundred simulated experiments.

A question arises on whether the present method could be effectively employed with a small number of atoms and a limited sampling of the interaction times. This is of course a crucial aspect concerning its possible implementation in a realistic scenario. We found, by means of an extensive set of simulated experiments, that the answer is positive and that accurate reconstructions may be obtained using realistic values of the parameters. In fig. 4 we report, as an example, the results of a simulated experiment, corresponding to that of fig. 2c, now performed with $n_\tau = 40$, $N_x = 30$ and $N_{\text{it}} = 50$. As it is apparent from the plots, the reconstruction is still very accurate despite the fact that the total number of observations has been dramatically decreased.

Error analysis. – The quality of the reconstruction is affected both by the accuracy of the experimental data and by the choice of the range of interaction times $[\tau_0, \tau_{n_\tau}]$ in which the atom statistics is sampled. The former is responsible for the fluctuations in the reconstructed distribution, whereas the latter affects the potential biasedness of the reconstruction. Let us first analyze the effect of the choice of the interval $[\tau_0, \tau_{n_\tau}]$. An extensive numerical analysis has shown that the optimal range is the one including as many as possible *neat* oscillations. In order to illustrate the point, let us focus on the specific example of the MA regime (fig. 2b, left plot): the last visible minimum of P_e is at $\tau \approx 4.3$. This is already quite blurred (the oscillations appearing after this one are *totally* blurred, so we did not

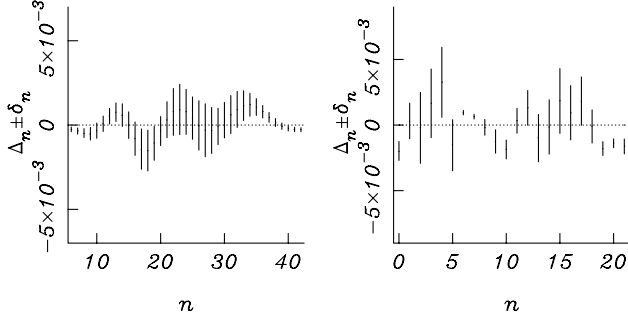Fig. 5: The absolute deviation Δ_n of the reconstructed distribution from the theoretical value together with the standard deviation of the mean δ_n. See the text for details. The left and right plots are obtained by $W = 10$ runs of the simulated experiments presented in fig. 2b and fig. 2c, respectively.

consider them in our analysis), but it is still crucial for a reliable reconstruction. In fact, the first steep and well-recognizable oscillations may be obtained *also* by means of photon distributions quite different from the actual one, whereas in order to describe also the small oscillations appearing as τ increases, one is led towards the actual distributions.

On the other hand, the fluctuations in the reconstructed distribution are essentially due to the fluctuations of the data themselves. The overall accuracy of the ML reconstruction can be estimated either by modeling the statistics of counts [20] or, more directly, by virtue of the central limit theorem, by repeated experiments. Let us denote by $p_n(h)$ the photon distribution as obtained by ML reconstruction in the h-th run. Then, the fluctuations of each run may be simply evaluated as the sample variance

$$\mathrm{Var}(p_n) = \frac{1}{W} \sum_{h=1}^{W} \left[p_n(h) - \langle p_n \rangle \right]^2, \tag{6}$$

where W is the number of runs and

$$\langle p_n \rangle = \frac{1}{W} \sum_{h=1}^{W} p_n(h)$$

is the total mean.

In order to assess statistical reliability and accuracy we compare the absolute deviations $\Delta_n = p_n - \langle p_n \rangle$ of the reconstructed distribution from the theoretical values p_n with the standard deviation of the mean $\delta_n \equiv \sqrt{\mathrm{Var}(p_n)/W}$. The results for the MA and DP cases, *i.e.*, the regimes with many-component photon distributions, are reported in fig. 5 for the simulated experiments described in fig. 2b and fig. 2c. As it is apparent from the plot, about 99% of the determinations are within two standard deviations from the theoretical value, thus confirming the statistical reliability of the method.

Another issue to be addressed is that concerning the choice of the truncation dimension $\tilde{n}$, which, in turn,

may be a relevant parameter for the reliability of the reconstruction procedure. Our strategy has been that of starting with a very large truncation dimension and then reducing it step by step until a loss of normalization has been reached. This procedure may be expensive in terms of computational resources, but ensures to circumvent the introduction of spurious information. On the other hand, a systematic analysis may be carried out analyzing the spectrum of the so-called G-operator [18].

Summary and conclusions. – We have suggested a novel iterative method to reconstruct the full photon distribution of the cavity field of a micromaser at the steady state starting from the statistics of the probe atoms leaving the cavity after different interaction times. Our methods works effectively using a small number of atoms and a limited sampling of the interaction times. This features, together with its accuracy and fast convergence, make it suitable for being used *on-line* with experiments. The method has been tested by numerically simulated experiments showing that it may be reliably used in any steady-state regime of the micromaser leading to high-fidelity reconstructions for single-peaked distributions as well as for double-peaked ones and for trapping states.

$$* * *$$

REFERENCES

[1] WALTHER H. *et al.*, *Rep. Prog. Phys.*, **36** (2006) 1325; HAROCHE S. and RAIMOND J. M., *Exploring the Quantum* (Oxford University Press, Oxford) 2006.
[2] MESCHEDE D. *et al.*, *Phys. Rev. Lett.*, **54** (1985) 551.
[3] JAYNES E. T. and CUMMINGS F. W., *Proc. IEEE*, **51** (1963) 89.
[4] REMPE G. *et al.*, *Phys. Rev. Lett.*, **64** (1990) 2783.
[5] REMPE G. *et al.*, *Phys. Rev. Lett.*, **58** (1987) 353.
[6] MEYSTRE P., REMPE G. and WALTHER H., *Opt. Lett.*, **13** (1988) 1078; WEIDINGER M. *et al.*, *Phys. Rev. Lett.*, **82** (1999) 3795.
[7] KOLOBOV M. I. and HAAKE F., *Phys. Rev. A*, **55** (1997) 3033; CASAGRANDE F., LULLI A. and ULZEGA S., *Phys. Rev. A*, **60** (1999) 1582.
[8] FILIPOWICZ P., JAVANAINEN J. and MEYSTRE P., *Phys. Rev. A*, **34** (1986) 3077; LUGIATO L. A., SCULLY M. O. and WALTHER H., *Phys. Rev. A*, **36** (1987) 740.
[9] VARCOE B. T. H. *et al.*, *Nature*, **403** (2000) 743; BRATTKE S. *et al.*, *Phys. Rev. Lett.*, **86** (2001) 3534.
[10] BRUNE M. *et al.*, *Phys. Rev. Lett.*, **59** (1987) 1899.
[11] AN K. *et al.*, *Phys. Rev. Lett.*, **73** (1994) 3375.
[12] REMPE G. and WALTHER H., *Phys. Rev. A*, **40** (1990) 1650; HERZOG U., *Phys. Rev. A*, **50** (1994) 783; CRESSER J. D. and PICKLES S. M., *Phys. Rev. A*, **50** (1994) R925.
[13] BRIEGEL H.-J. *et al.*, *Phys. Rev. A*, **49** (1994) 2962.

[14] SCULLY M. O. *et al.*, *Phys. Rev. A*, **44** (1991) 5992; CASAGRANDE F. *et al.*, *Phys. Rev. Lett.*, **90** (2003) 18.

[15] BANASZEK K., *Acta Phys. Slov.*, **47** (1997) 1; *Phys. Rev. A*, **57** (1998) 5013.

[16] MOGILEVTSEV D., *Opt. Commun.*, **156** (1998) 307; *Acta Phys. Slov.*, **49** (1999) 743.

[17] ZAMBRA G. *et al.*, *Phys. Rev. Lett.*, **95** (2005) 063602.

[18] HRADIL Z. *et al.*, *Phys. Rev. Lett.*, **96** (2006) 230401.

[19] ROSSI A. R. *et al.*, *Phys. Rev. A*, **70** (2004) 055801.

[20] HRADIL Z. and ŘEHÁČEK J., *Fortschr. Phys.*, **49** (2001) 1083.